Environ. Sci. Technol. **2006**, *40,* 3595−3602

Measuring Hydrophobic Micropore Volumes in Geosorbents from Trichloroethylene Desorption Data

HEFA CHENG AND MARTIN REINHARD*

Department of Civil and Environmental Engineering, Stanford University, Stanford, California 94305-4020

Hydrophobic micropores can play a significant role in controlling the long-term release of organic contaminants from geosorbents. We describe a technique for quantifying the total and the hydrophobic mineral micropore volumes based on the mass of trichloroethylene (TCE) sorbed in the slow-releasing pores under dry and wet conditions, respectively. Micropore desorption models were used to differentiate the fast- and slow-desorbing fractions in desorption profiles. The micropore environment in which organic molecules were sorbed in the presence of water was probed by studying the transformation of a water-reactive compound (2,2-dichloropropane or 2,2-DCP). For sediment from an alluvial aquifer, the total and hydrophobic micropore volumes estimated using this technique were 4.65 μL/g and 0.027 μL/g (0.58% of total), respectively. In microporous silica gel A, a hydrophobic micropore volume of 0.038 μL/g (0.035% of reported total) was measured. The dehydrohalogenation rate of 2,2-DCP sorbed in hydrophobic micropores of the sediment was slower than that reported in bulk water, indicating an environment of low water activity. The results suggest that hydrolyzable organic contaminants sorbed in hydrophobic micropores react slower than in bulk water, consistent with the reported persistence of reactive contaminants in natural soils.

Introduction

Adsorption in micropores (pores with diameters <2 nm) of geosorbents (soils and sediments) is an important factor influencing the fate and transport of hydrophobic organic contaminants in the subsurface environment (*1*−*4*). At high concentrations, sorption and desorption of volatile organic compounds (VOCs) is typically fast and dominated by organic matter, whereas at low concentrations, release from geosorbents (especially when aged) can be very slow. The slow desorption has been attributed to adsorption and slow diffusion in micropores (*2*, *4*−*6*). The contaminant flux desorbing from micropores over a long period can result in significant groundwater contamination, especially for compounds with low maximum contaminant levels, such as 1,2-dibromoethane and vinyl chloride. Strong sequestration of organic contaminants in micropores can make sorption appear irreversible (*3*, *5*) and significantly reduce bioavailability (*7*, *8*).

Studies have shown that desorption of VOCs from wet microporous sorbents occurs in two distinct stages: a first stage that lasts minutes to hours with a relatively rapid removal rate, and a second stage with a distinctly slower desorption rate that lasts on the order of weeks to years (*1*−*3*). If the initial VOC mass is relatively high, most of it is removed as the fast-desorbing fraction in the first stage where the desorption rate may be controlled by retarded diffusion through water-filled mesopores (2−50 nm) (*3*). During the second stage when the desorption rate is distinctly slower, mass transfer is believed to be limited by diffusion through hydrophobic micropore spaces (*3*, *9*). A radial diffusion model, either by itself or coupled with the advection-dispersion equation, has been used by Li and Werth to describe the desorption characteristics of microporous sorbents packed in columns (*4*). This model does not consider "slow" desorption processes occurring outside of micropores (e.g., desorption from external surface), and therefore does not allow evaluation of micropore diffusion separately in the first desorption stage.

Micropores may be present in the surface microstructures of minerals resulting from weathering, precipitation, and turbostratic stacking of nanosized particles and in the forms of nanoscale structural pores, cavities, and channels in both crystalline and amorphous minerals (*10*). A recent study observed a linear relationship between the microporosity of soils and their clay contents and concluded that the micropores are located mainly in the clay fraction (*11*). A schematic illustration of the formation of micropores in clay minerals is shown in the Supporting Information (Figure S1). Properties such as composition, charge, adsorbed ions, and functional groups determine the polarity of mineral surfaces and thus the adsorption of water and hydrophobic compounds. Polar surfaces are deactivated by the strong adsorption of water, which prevents significant sorption of hydrophobic compounds. By contrast, hydrophobic solutes can outcompete water on hydrophobic surfaces that interact only weakly with water due to the hydrophobic effect. In mineral micropores, we expect this behavior to be more pronounced: water is tightly bound in polar micropores and is difficult to displace, while in hydrophobic pores water is weakly bound and displaceable by organic compounds. To predict the fate and transport of organic contaminants, it is important to know the volumes of hydrophobic micropores in geosorbents. Although the significance of geosorbent microporosity on contaminant behavior has been well documented (*1*, *2*, *3*, *12*), there is no established method for quantifying the effective (hydrophobic) micropore volume under natural conditions.

The most prevalent technique for characterizing microporous materials is low-temperature gas adsorption, in which a gas (usually nitrogen) at its boiling point is adsorbed on the solid sample that has been degassed at an elevated temperature and under vacuum. Micropore size distribution and volume are calculated from the acquired isotherm data by using the Dubinin−Radushkevich, Horvath−Kawazoe, Dubinin-Astakhov, or other methods (*13*). However, results of gas adsorption are not applicable to predict organic sorption in the presence of water because water strongly competes for sorption sites and reduces the volume of micropores accessible to organic molecules. Because geosorbents are typically moist in natural settings, we hypothesize that only the hydrophobic micropores are relevant for understanding the sorption behaviors of hydrophobic contaminants.

The fact that water is a less effective competitor for sorption in hydrophobic micropores implies that the hydrophobic organic molecules are not fully surrounded by water molecules in such pores, as they would be in solutions. Therefore, it is further hypothesized that the reactions of

* Corresponding author phone: (650)723-0308; fax: (650)723-7058; e-mail: reinhard@stanford.edu.

10.1021/es0522581 CCC: $33.50
Published on Web 04/22/2006

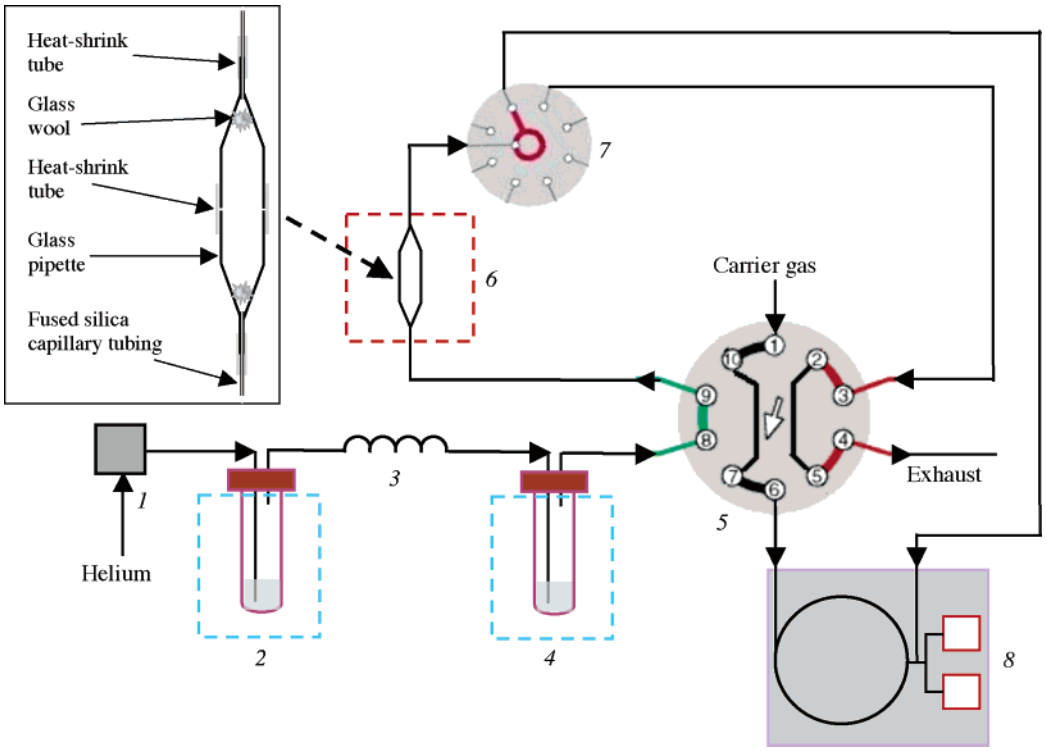

FIGURE 1. Flow diagram of the column apparatus used for measuring sorption and desorption kinetics: [1]digital mass flow controller, [2]organic vapor saturator immersed in refrigerated bath, [3]extra fused silica coil, [4]water vapor saturator immersed in water bath, [5]10-port 2-position injection valve, [6]sorption column (~1.1 cm^3) housed in a GC oven, [7]8-port dead-end switching valve, and [8]GC with FID and ECD detectors (linked to a computer).

organic contaminants with water are inhibited by micropore sorption. To evaluate this hypothesis, we chose to study the pH-independent dehydrohalogenation of 2,2-dichloropropane (2,2-DCP), which is promoted by water (*14*). The reaction proceeds via the E_1 mechanism (*15*):

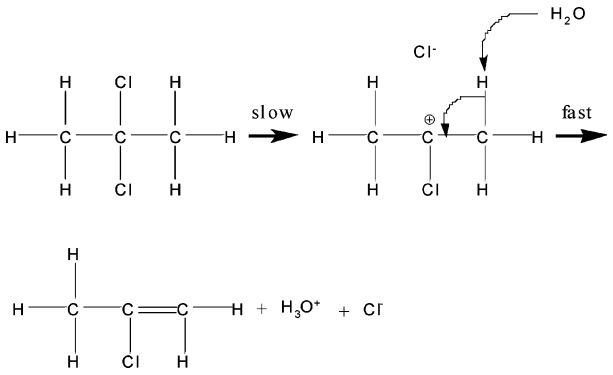

Although the rate of this unimolecular reaction depends only on 2,2-DCP concentration in aqueous solutions, in hydrophobic micropores where the activity of water (and OH^-) is low, 2,2-DCP transformation is expected to be slower.

In this paper, we describe an apparatus that can measure the sorption and desorption kinetics of VOCs on microporous solids on the time scales of seconds to weeks under environmentally relevant conditions. The total and hydrophobic micropore volumes of model solids were inferred from the slow-desorbing masses, which were quantified from desorption flux data evaluated by micropore desorption models. The hydrophobicity of micropores was also probed by studying the dehydrohalogenation of sorbed 2,2-DCP molecules. This study is a first attempt to quantify the volume of hydrophobic micropores that are accessible to hydrophobic organic molecules even in the presence of water. Results indicate that organic molecules can outcompete water for sorption in the hydrophobic micropores, and hydrolyzable molecules residing in such pores react with water at a slower rate than in bulk solution.

Materials and Method

The experimental apparatus consisted of a vapor generator, sorption column, and a detection system, as shown in Figure 1. Helium (99.996%) supplied from a cylinder with two moisture traps was regulated by a digital mass flow controller (Cole-Parmer, Vernon Hills, IL). Organic vapor was generated by bubbling helium through liquid contained in the organic vapor saturator, which was cooled in a refrigerated bath. The coil that follows equilibrated the exiting gas stream to the ambient temperature. The relative humidity (RH) was controlled by bubbling the gas stream through water in the water vapor saturator immersed in a temperature-controlled water bath. The RH in the gas stream corresponded to the water vapor pressure at the bath temperature and was calibrated with a humidity sensor. The vapor saturators were adapted from capillary column washers (Alltech, Deerfield, IL), and all flow lines were made of 0.53 mm o.d. fused silica capillary tubing (Supelco, St. Louis, MO).

The sorption column was made by joining two truncated glass pipets and was housed inside a GC oven to maintain constant temperature (24−300 °C). The small ends of the pipets were connected to the capillary tubing by 0.91 mm i.d. fluoroplastic PTFE/FEP dual shrink tubing, while the large ends were jointed (without heating) together by 6.1 mm i.d. double-walled PTFE heat-shrink tubing after the sorbent was packed. A switching valve and an injection valve (Valco, Houston, TX) were used to switch flow paths and to inject gas samples. Organic concentrations in the gas phase were analyzed by an HP 5890 II GC equipped with a FID and an ECD connected in parallel. The apparatus was operated either in continuous sampling mode when column effluent was introduced directly to the detectors or in discrete sampling

TABLE 1. Best-Fit Micropore Diffusion Rate Constants (D/R^2) and Shape Factors (η) for TCE Desorption from the Silica Gel and LLNL Sediment (at 24 °C) and the Micropore Volumes Calculated from Experimental Data

solid and condition	first desorption stage[a] D/R^2 (min^{-1})	second desorption stage[b] D/R^2 (min^{-1})	η	micropore volume[c] (μL/g)
dry silica gel	4.20×10^{-3}	1.81×10^{-4}	8.97	N/A[d]
wet silica gel	7.90×10^{-3}	3.70×10^{-4}	0.72	0.038
dry LLNL sediment	1.19×10^{-1}	4.09×10^{-4}	1.32	4.65
partially wet LLNL sediment	4.45×10^{-2}	6.04×10^{-4}	0.88	0.027
wet LLNL sediment	5.90×10^{-3}	6.00×10^{-4}	2.28	0.027

[a] Obtained by fitting experimental data with a radial diffusion model coupled with the advection-dispersion equation, where D/R^2 actually accounts for the collective contributions from the "slow" desorption of molecules residing outside of micropores and micropore diffusion. [b] Obtained by fitting experimental data with a radial diffusion model alone, and a γ distribution of diffusion rate constants was assumed to account for desorption from micropores with a wide distribution of sizes and properties, where D/R^2 is the mean micropore diffusion rate constant and η is the shape factor. [c] Calculated from TCE mass remaining after the first desorption stage with the assumption that TCE molecules resided in micropores at the same density as under standard conditions. [d] N/A—method does not apply because a significant amount of TCE also desorbed from micropores in the first desorption stage.

mode with samples of column influent and effluent injected alternately into the GC column. The detectors were calibrated by introducing doses of organic vapor obtained by combinations of refrigerated bath temperature and sampling loop size of the injection valve. Relationships between temperature and organic vapor concentration were obtained from the Antoine equations (*16*). It was observed that organic vapor in the gas stream was always in equilibrium with the cooled organic liquid under experimental conditions (data not shown).

We chose silica gel A and the clay and silt fraction (<75 μm) of sediment from an alluvial aquifer in Lawrence Livermore National Laboratory (LLNL), which had been studied in previous works (*3*, *17*), as model and reference solids. LLNL sediment has an organic carbon content of 0.11% (*17*), and our X-ray diffraction analyses show that it is mainly composed of quartz, albite, montmorillonite, and kaolinite (data not shown). Dry solids were dehydrated in a 105 °C oven for 48 h. Wet solids were prepared by equilibrating (>3 months) dry solids at 100% RH above water in desiccators at room temperature (24±1 °C), thereby coating surfaces with a film of water and filling pores up to 100 nm radius through capillary condensation (*1*, *2*). Sorption of VOCs in micropores of such wet solids has been found to be identical to that in saturated aqueous systems (*1*, *2*, *12*). A partially wet LLNL sediment sample was also prepared by equilibration at ~38% RH controlled by a saturated NaI solution (*18*). Dehydration at 105 °C for 48 h indicates that water contents of the partially wet and wet sediments were 26 and 54 mg/g, respectively. TCE was selected as a nonreactive sorbate, while 2,2-DCP was chosen because it dehydrochlorinates with a half-life ($t_{1/2}$=39.5 h at 24 °C) that is suitable for this study, and the reaction is pH-independent (*15*).

Masses of solids packed in columns were determined from the column weight differences before and after packing. Dry solid columns were baked in a 105 °C oven, while those containing partially wet and wet solids were reconditioned in a humidified (38% or 100% RH) helium stream for at least 2 h. During sorption, a humidified (38% or 100% RH) helium stream containing TCE or 2,2-DCP vapor was fed to the column packed with the partially wet or wet solids at 1.00 mL/min, with the organic concentration controlled by the refrigerated bath temperature. For sorption on dry solids, the water vapor saturator was removed. Sorptive uptake was quantified by measuring the effluent concentration in continuous sampling mode until full breakthrough. The column was then disconnected, sealed, and incubated in a 50 °C oven. The organic vapor saturator was also disconnected, and the water vapor saturator was replaced by one that contained pure water. After being incubated for 10 h, the column was cooled to room temperature, reconnected to the flow path, and purged by humidified (38% or 100% RH) helium at 1.00 mL/min (equivalent to a flow rate of ~1.4 pore volume/min). The fast TCE concentration decline at the beginning of desorption was captured by continuous sampling, while the more gradual changes later in the desorption experiment were measured discretely. The flow out of the 2,2-DCP column was sampled discretely to quantify both 2,2-DCP and 2-CP. Step increases in the column temperature were made after the desorbed flux was relatively low to accelerate desorption (*3*, *19*).

Breakthrough curves and desorption profiles were integrated to evaluate mass balances. Quantitative analysis of experimental data was performed using the approaches of Li and Werth (*4*), and more details are given in the Supporting Information. The first desorption stage of the mass remaining profiles was modeled using a radial diffusion model (with a single diffusion rate) coupled with the advection-dispersion equation, while the second desorption stage was modeled by a radial diffusion model with a γ distribution of diffusion rate constants. Modeling served (1) to identify the beginning of the slow-desorbing fraction and (2) to evaluate micropore diffusion rates in the second desorption stage, which allowed comparison with published values. Micropore diffusion rate constants (D/R^2) and shape factors (η) obtained from the best model fits for experimental data are listed in Table 1. Micropore volumes (Table 1) were calculated from the slow-desorbing masses based on the Gurvitsch rule, which states that the total micropore volume is independent of the adsorbate provided that the amount adsorbed is expressed as the liquid volume and that selective effects are absent (*13*).

Results and Discussion

1. Slow and Fast TCE Desorption from Silica Gel and LLNL Sediment. Figure 2a shows TCE mass remaining profiles of the wet and dry silica gels along with the model fits, and Table 1 summarizes the best-fit micropore diffusion rate constants. In both cases, the two-stage desorption behavior characteristic of microporous solids (*1*−*4*) was observed, and the first desorption stages could be fitted by a radial diffusion model coupled with the advection-dispersion equation. Most of the mass was removed during the first stages in which TCE concentrations decreased by more than 2 orders of magnitude (Figure S2, Supporting Information). During the second desorption stages, when the interstitial TCE vapor concentrations approached zero, mass transfer limitations external to solid particles were no longer significant. To describe TCE desorption under this condition, a radial diffusion model with a γ distribution of diffusion rate constants was invoked. Increasing the column temperature led to short-term desorption flux increases (Figure S2,

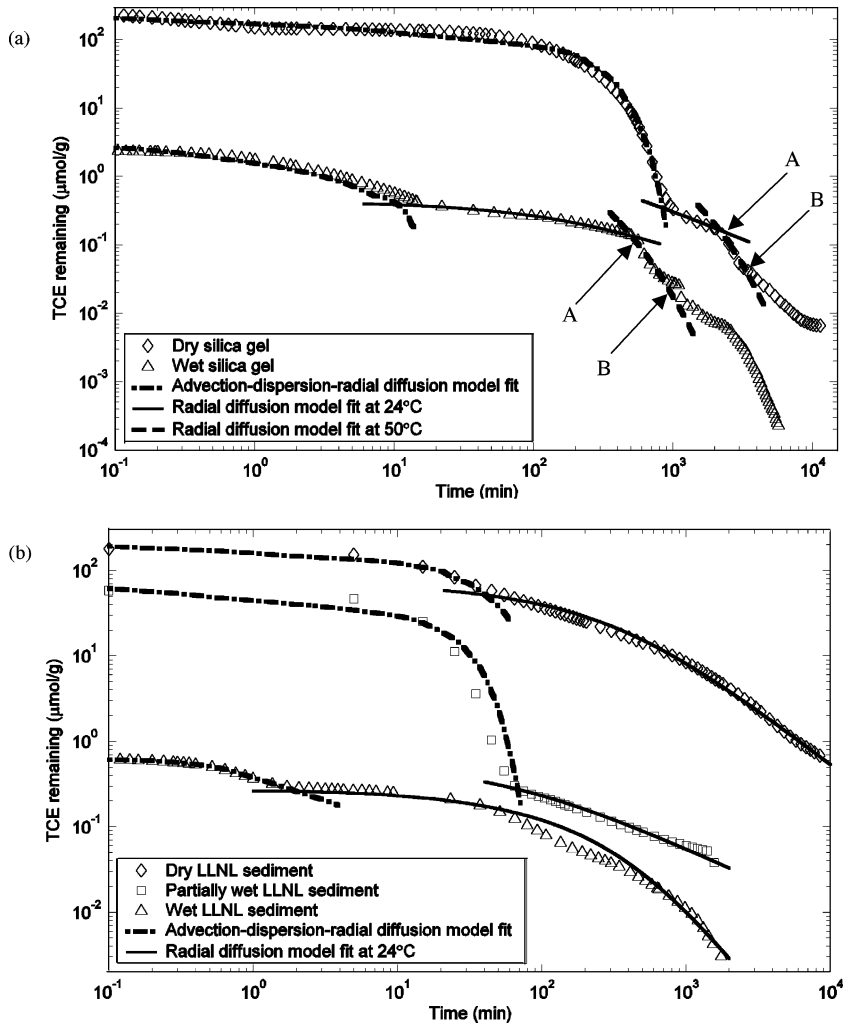

FIGURE 2. TCE mass remaining on (a) dry and wet silica gels and (b) dry, partially wet, and wet LLNL sediments. For the silica gels, desorption temperature was increased stepwise from 24 °C to 50 °C (points A) and to 75 °C (points B). Further temperature increases (model fittings not shown) were also made in 25 °C increments, as shown in the Supporting Information (Figure S2). Only partial data are shown in (a) and (b).

Supporting Information), as expected, and this effect could be accounted for by higher micropore diffusion rates.

In wet silica gel, the first desorption stage lasted 14.5 min (~20 pore volumes), longer than the expected time to remove TCE molecules adsorbed on the external surfaces and at the water−gas interface, partitioned in the adsorbed water, and resided in the large interparticulate void space. The advection-dispersion-radial diffusion model adequately described this stage, but the high D/R^2 (7.90×10^{-3} min^{-1}) indicated the existence of hindered desorption mechanisms. The exact nature of these "slow" processes are not clear but could be caused by desorption of TCE molecules adsorbed on the hydrophobic surfaces and retarded diffusion through water-filled mesopores (*3*). Because duration of the first desorption stage was relatively short, the contribution of TCE desorbed from micropores was assumed to be small. The mass removed in the second desorption stage corresponded to TCE desorbed from the hydrophobic micropores of the wet silica gel, which was 0.42 μmol/g.

In dry silica gel, the total amount of TCE sorbed was 247 μmol/g, more than 100 times larger than that in wet silica gel. The first desorption stage lasted approximately 1000 min, which was ~70 times longer than that in wet silica gel. The high desorption fluxes observed (Figure S2b, Supporting Information) and the large amount of TCE desorbed (99.5 μmol, equivalent to filling of 2.5% of the total pore space (0.87 mL/g) (*12*)) could not be explained by the desorption of surface-adsorbed TCE alone. Although D/R^2 (4.20×10^{-3} min^{-1}) of the first desorption stage was within the range reported for micropore diffusion (*4*), it probably reflected the rates of TCE desorbing from strongly sorbing silica gel surfaces and retarded diffusion through relatively large micropores. In the second desorption stage, external mass transfer limitations were negligible, and the much smaller D/R^2 (1.81×10^{-4} min^{-1}) was indicative of TCE transport through smaller size micropores. Because significant micropore desorption occurred during both stages in dry silica gel, TCE mass desorbed in the second stage cannot be used to estimate the total micropore volume. Such two-stage micropore desorption behavior has been observed on zeolites with nonuniform pore sizes (*4*).

Experimental and model-fitted mass remaining profiles of TCE on the dry, partially wet, and wet LLNL sediments are presented in Figure 2b, and their micropore diffusion rate constants are included in Table 1. As in the dry and wet silica gels, desorption occurred in two stages in all cases. The uptake of TCE by dry, partially wet, and wet sediments decreased from 178, to 58, and to 0.62 μmol/g with increasing water content (0, 26, and 54 mg/g, respectively). This was attributed to the strong competition of water molecules for surface sites and spaces in micropores. Removal of fast-desorbing TCE from the wet sediment occurred within 2 min (~2.8 pore

volumes), and the contribution from micropore desorption was negligible in this fraction. The relatively large micropore diffusion rate (5.90×10^{-3} min^{-1}) suggested that removal of TCE molecules residing outside of micropores was also hindered, probably by sorption on hydrophobic surfaces and diffusion through water-filled mesopores. For the dry sediment, the first desorption stage lasted ~50 min with a D/R^2 (1.19×10^{-1} min^{-1}) 20 times higher than that in wet sediment, which was too high to be attributable to micropore diffusion. Instead, the flux desorbed during this stage was interpreted as TCE desorption from the dry sediment surfaces. The slow desorption from micropores only contributed to a small fraction of the TCE removed in this stage. TCE desorption behavior from the partially wet sediment was between those from the wet and dry ones. Equilibration at 38% was expected to fill at least all hydrophilic micropore spaces and cover the polar regions of external surfaces on LLNL sediment by water. In the first desorption stage, D/R^2 (4.45×10^{-2} min^{-1}) of the partially wet sediment was also between the values of the dry and wet ones, consistent with the diminishing influence of external surface on TCE adsorption with increasing RH. The distinct transition between the first and second desorption stages occurred once micropore desorption started to dominate desorbed TCE flux.

Micropore diffusion rates in the second desorption stages of the partially wet (D/R^2=6.04×10^{-4} min^{-1}) and wet (D/R^2=6.00×10^{-4} min^{-1}) sediment samples were almost identical, consistent with complete filling of the micropores at 38% RH. TCE masses remaining in the dry, partially wet, and wet sediments after the first desorption stage were 51.7, 0.30, and 0.30 μmol/g, respectively. The fact that the partially wet and wet sediments sorbed the same amount of TCE in their micropores also consistently indicated that TCE only sorbed in hydrophobic micropores with all hydrophilic ones being water-filled. Taken together, these data support the hypothesis that in silica gel and LLNL sediment water is a strong competitor for hydrophilic micropores, but it competes only weakly for spaces in hydrophobic micropores.

Because TCE desorption rate in the second desorption stage is solely controlled by micropore diffusion, D/R^2 and η for this stage are taken as indicative of the physical micropore characteristics. The only exception is on the dry silica gel, where D/R^2 values in the first and second stages are believed to represent mostly the significantly different diffusion rates in micropores of different sizes. Diffusion rates of TCE in micropores of the silica gel and LLNL sediment listed in Table 1 are comparable to the reported values (*4*). It also shows that D/R^2 values (second desorption stage) are lower under wet conditions than dry, which be explained by stronger interactions of TCE molecules with the micropore wall surfaces in the absence of water. η describes the distribution of the micropore diffusion rate constant, and the wet solids tended to have a lower η compared to the dry ones. For the partially wet (η=0.88) and wet (η=2.28) LLNL sediments, the shape factors differed by a factor 2.6. Without additional information, however, these differences are difficult to interpret.

2. Applicability of Desorption Method for Quantifying Hydrophobic Micropore Volume. Limited data are available to validate the TCE desorption technique for quantifying total microporosity, whereas no methods have been reported to quantify hydrophobic micropore volume. For the silica gel, gas adsorption indicates a total micropore volume of 108.8 μL/g (*12*), and the TCE desorption technique (under wet conditions) employed here suggests that a very small fraction of the total micropore volume, 0.035%, or 0.038 μL/g, is hydrophobic. For dry LLNL sediment, the reported total microporosity is below the instrument detection limit (0.1 μL/g) of gas adsorption (*12*), whereas TCE desorption (under dry conditions) in this study indicates a micropore volume of 4.65 μL/g. This discrepancy is possibly due to pore structure changes caused by vacuum-degassing at elevated temperatures applied in gas adsorption, which has been found to cause significant particle rearrangement and destruction of microporosity in clay minerals (*20*, *21*). The total micropore volume of LLNL sediment measured by the TCE desorption technique is comparable to the microporosity determined by argon adsorption for low organic geosorbents that were vacuum-degassed at 60 °C (*6*). TCE desorption from the partially wet and wet LLNL sediments suggests a hydrophobic micropore volume of 0.027 μL/g, which is 0.58% of the total micropore volume. The data obtained here indicate that the TCE desorption technique should be applicable to the determination of the total microporosity in geosorbents and especially to the determination of the hydrophobic micropore volume in the presence of water, a property that has so far not been measured.

The fact that the micropores in LLNL sediment are predominantly hydrophilic is consistent with the polar nature of most mineral surfaces. In the case of micropores formed by stacking of clay plates (Figure S1, Supporting Information), all micropores are hydrophilic with the exception of those surrounded by uncharged siloxane surfaces, which are hydrophobic (*22*, *23*). It has been observed that smectites with relatively hydrophobic siloxane surfaces could retain large amounts of phenanthrene from water, an effect that was attributed to capillary condensation into a network of micropores created by quasicrystals or tactoids of clay (*24*). This agrees with the mechanism proposed here for VOC sorption in hydrophobic micropores. Although the volume of hydrophobic micropores is likely small in geosorbents, they can play significant roles in the uptake and slow release of hydrophobic compounds.

Currently, little is known about the contribution of different geosorbent components to the total and hydrophobic microporosity. Carbonaceous particles and soil organic matter also exhibit microporosity, and they are strong sorbents for organic contaminants (*25*–*27*). Micropore volumes ranging from 14 to 127 μL/g have been reported (*25*, *27*), which indicate that the organic fraction is much more microporous than the mineral fraction in geosorbents. Because their micropores are likely hydrophobic, small quantities of carbonaceous materials (e.g., >1%) could possibly dominate the slow sorption and desorption behavior of organic contaminants.

3. Micropore Environment Probed by 2,2-DCP Transformation. Transformation of 2,2-DCP was studied to evaluate the hypothesis that hydrolyzable organic compounds that sorbed in hydrophobic micropores by displacing water react with water at a slower rate than in bulk solution. Figure 3a shows the concentration profiles of 2,2-DCP and 2-CP desorbed from a column packed with wet LLNL sediment, which had been loaded with 3.76 μmol of 2,2-DCP before incubation. During desorption, 2,2-DCP concentration decreased rapidly to ~0.1 μmol/L in 15 min, then it decreased more gradually, and finally remained at ~0.03 μmol/L. The desorption profile indicates that the masses desorbed after 15 min came from the micropores. The temperature increase at ~1600 min had a negligible effect on 2,2-DCP desorption flux, suggesting that 2,2-DCP was nearly depleted. The behavior of 2-CP differed in that its concentration decreased almost exponentially before reaching 0.05 μmol/L. Thereafter, 2-CP concentration decreased slowly and went below detection at ~1400 min.

Figure 3b shows the cumulative masses of 2,2-DCP and 2-CP removed from the column. A relatively large amount of 2,2-DCP (0.30 μmol) desorbed in the fast-desorbing fraction, while the flux of 2,2-DCP desorbed from the micropores was low but steady, which suggests that a fraction of the 2,2-DCP molecules sorbed in the hydrophobic mi-

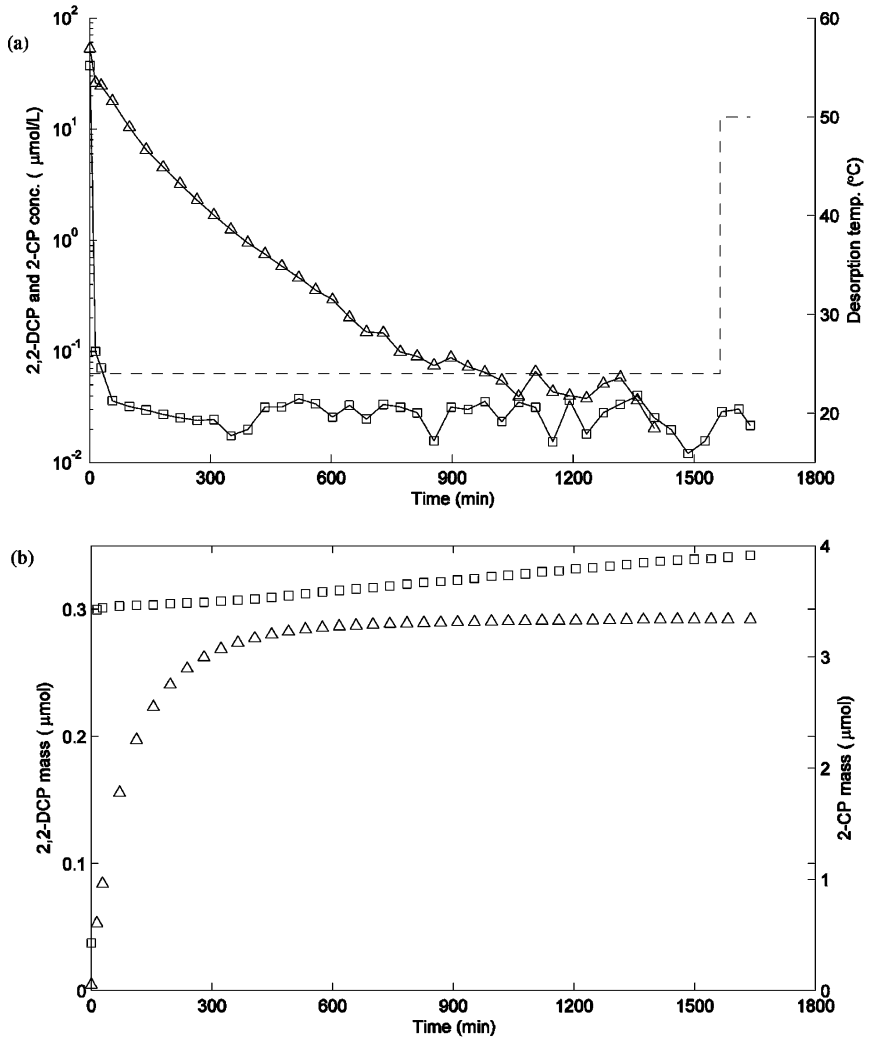

FIGURE 3. Desorption of 2,2-DCP (□) and 2-CP (△) from the wet LLNL sediment after incubation at 50 °C for 10 h: (a) 2,2-DCP and 2-CP concentrations in the purge flow plotted as a function of time with desorption temperature (- -) shown on the secondary *Y* axis and (b) cumulative masses of 2,2-DCP and 2-CP removed during desorption.

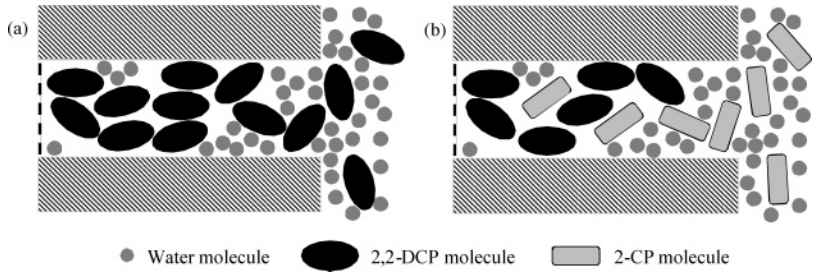

FIGURE 4. Schematic illustration of sorption and dehydrohalogenation of 2,2-DCP molecules in a slit-shaped, hydrophobic micropore: (a) water molecules occupying the hydrophobic micropore spaces have rather weak interactions with the hydrophobic pore wall surfaces, and they are displaced by the incoming 2,2-DCP molecules and (b) after a long reaction time, 2,2-DCP molecules residing outside of the micropore with ready access to water undergo dehydrohalogenation, while some 2,2-DCP molecules in the hydrophobic micropore are preserved because of limited contact with water molecules.

cropores had been protected from reaction with water. The micropore volume occupied by the unreacted 2,2-DCP (in the slow-desorbing fraction) was only 0.0031 μL/g, much lower than the hydrophobic micropore volume (0.027 μL/g). This could be partially explained by transformation of sorbed 2,2-DCP in the hydrophobic micropores. In contrast, only a small fraction (18.1%) of the total mass of 2-CP desorbed was removed in the fast-desorbing fraction. The continuous decrease in 2-CP concentration during desorption suggests that the rate of 2,2-DCP dehydrohalogenation was slower deeper in the micropores.

2,2-DCP undergoes dehydrohalogenation in bulk water at a rate of 2.93×10^{-4} min^{-1} at 24 °C, with a reaction activation energy of 111.1 ± 2.0 kJ/mol (*14*). At 50 °C, $t_{1/2}$ of 2,2-DCP in bulk water is reduced from 39.5 h (24 °C) to 1.06 h, and the calculated residual 2,2-DCP in a solution after 10 h is 0.0052%. Desorption at room-temperature lasted for 25.5 h (0.65 $t_{1/2}$), while 2-CP was not detected during the desorption at 50 °C. Consequently, 2,2-DCP could be approximated as being nonreactive during desorption, and the masses of 2,2-DCP and 2-CP desorbed represented the residuals after incubation. Evaluation of the masses desorbed indicates that

97.8% of the sorbed mass was accounted for: 0.34 μmol as 2,2-DCP and 3.34 μmol as 2-CP. Of the 2,2-DCP originally sorbed in the hydrophobic micropores (from 2,2-DCP and 2-CP desorbed in the slow-desorbing fraction), 1.54% remained unreacted, significantly more than the 0.0052% predicted from the rate in homogeneous solution. This inhibition on dehydrohalogenation of 2,2-DCP sorbed in micropores is consistent with the hypothesis that organic molecules sorbed in hydrophobic micropores are exposed to water of lower activity.

Experimental results from this study consistently suggest that small organic compounds, such as TCE and 2,2-DCP, can access the hydrophobic micropores in the presence of water. Water-reactive solutes (e.g., 2,2-DCP) are transformed while residing in hydrophobic micropores but at a slower rate than in bulk water. Figure 4 illustrates this inhibition effect by sorption in hydrophobic micropores. The water-reactive 2,2-DCP molecules have limited contact with water molecules in the hydrophobic micropores and consequently hydrolyze more slowly. Studies have shown that the pH-independent hydrolyses of organophosphorothiate esters and haloalkanes were unaffected by sorption on low-carbon sediments (*28*, *29*). However, within the confined space of hydrophobic micropores, dehydrohalogenation of 2,2-DCP molecules may be limited by the availability of nucleophiles (H_2O and OH^-) in the surroundings. We interpret the inhibition effect of micropore sorption on hydrolysis as caused by exclusion of weakly sorbed water by hydrophobic compounds in hydrophobic micropores, although other explanations cannot be ruled out. This mechanism is consistent with the high exothermic adsorption enthalpies observed for TCE sorption in silica gels, which indicated that TCE adsorption was occurring in hydrophobic micropores with the concomitant displacement of water (*30*).

Implications for Environmental Fate and Transport

Results from this study imply that only a small fraction (<1%) of the micropores in the silica gel and LLNL sediment are hydrophobic and that hydrophobic compounds sorbed in them effectively compete with water and are partially excluded from reaction with water. This agrees with the conclusion from a thermodynamic investigation of TCE sorption in water-saturated microporous sorbents (*30*) and the reported persistence of 1,2-dibromoethane, a water-reactive pesticide that has been found to be preserved in soils much longer than predicted from the bulk water hydrolysis rate (*5*). The fact that contaminants sequestered in hydrophobic micropores are not displaced by water has important implications for developing cleanup technologies and predicting the efficacy of natural attenuation of contaminated sites. Given the particle sizes (<75 μm) of the LLNL sediment studied, the rate of diffusion from its micropores is in the range of 10^{-8}–10^{-11} cm^2/s, much smaller than those (10^{-6}–10^{-5} cm^2/s) of small organic nonelectrolytes in water (*5*). It should be noted that the time scale for diffusion at the particle scale (days to weeks) is too short to explain the persistence of these chemicals in groundwater and soils, which can be on the order of years. To evaluate the significance of hydrophobic micropores as contaminant sinks and sources at contaminated sites, one also needs to consider transport phenomena at the relevant scale.

Acknowledgments

This study was funded by the U.S. Environmental Protection Agency under project R828772-01 through the Western Region Hazardous Substance Research Center. We thank Jian Luo and Yuanan Hu for their help with numerical modeling and anonymous reviewers for very helpful comments.

Supporting Information Available

Additional information on micropore formation in clay minerals; micropore desorption models and simulation approaches; and desorbed TCE concentration profiles from the wet and dry silica gels. This material is available free of charge via the Internet at http://pubs.acs.org.

Literature Cited

(1) Grathwohl, P.; Reinhard, M. Desorption of trichloroethylene in aquifer material: rate limitation at the grain scale. *Environ. Sci. Technol.* **1993**, *27* (12), 2360–2366.

(2) Farrell, J.; Reinhard, M. Desorption of halogenated organics from model solids, sediments, and soil under unsaturated conditions. 2. Kinetics. *Environ. Sci. Technol.* **1994**, *28* (1), 63–72.

(3) Werth, C. J.; Reinhard, M. Effects of temperature on trichloroethylene desorption from silica gel and natural sediments. 2. Kinetics. *Environ. Sci. Technol.* **1997**, *31* (3), 697–703.

(4) Li, J.; Werth, C. J. Slow desorption mechanisms of volatile organic chemical mixtures in soil and sediment micropores. *Environ. Sci. Technol.* **2004**, *38* (2), 440–448.

(5) Steinberg, S. M.; Pignatello, J. J.; Sawhney, B. L. Persistence of 1,2-dibromoethane in soils: entrapment in intraparticle micropores. *Environ. Sci. Technol.* **1987**, *21* (12), 1201–1208.

(6) Li, J.; Werth, C. J. Evaluating competitive sorption mechanisms of volatile organic compounds in soils and sediments using polymers and zeolites. *Environ. Sci. Technol.* **2001**, *35* (3), 568–574.

(7) Pignatello, J. J.; Xing, B. Mechanisms of slow sorption of organic chemicals to natural particles. *Environ. Sci. Technol.* **1996**, *30* (1), 1–11.

(8) Chung, N.; Alexander, M. Effect of soil properties on bioavailability and extractability of phenanthrene and atrazine sequestered in soil. *Chemosphere* **2002**, *48* (1), 109–115.

(9) Weber, W. J., Jr.; Huang, W. A distributed reactivity model for sorption by soils and sediments: 4. Intraparticle heterogeneity and phase-distribution relationships under nonequilibrium conditions. *Environ. Sci. Technol.* **1996**, *30* (3), 881–888.

(10) *Soil Mineralogy with Environmental Applications*; Dixon, J. B., Schulze, D. G., Eds.; Soil Science Society of America, Inc.: Madison, WI, 2002; p 866.

(11) Aringhieri, R. Nanoporosity characteristics of some natural clay minerals and soils. *Clays Clay Miner.* **2004**, *52* (6), 700–704.

(12) Werth, C. J.; Reinhard, M. Effects of temperature on trichloroethylene desorption from silica gel and natural sediments. 1. Isotherms. *Environ. Sci. Technol.* **1997**, *31* (3), 689–696.

(13) Gregg, S. J.; Sing, K. S. W. *Adsorption, Surface Area and Porosity*; Academic Press: London, 1982; p 303.

(14) Jeffers, P. M.; Ward, L. M.; Woytowitch, L. M.; Wolfe, N. L. Homogeneous hydrolysis rate constants for selected chlorinated methanes, ethanes, ethenes, and propanes. *Environ. Sci. Technol.* **1989**, *23* (8), 965–969.

(15) Roberts, A. L.; Jeffers, P. M.; Wolfe, N. L.; Gschwend, P. M. Structure–reactivity relationships in dehydrohalogenation reactions of polychlorinated and polybrominated alkanes. *Crit. Rev. Environ. Sci. Technol.* **1993**, *23* (1), 1–39.

(16) *Lange's Handbook of Chemistry,* 15th ed.; Dean, J. A., Ed.; McGraw-Hill: New York, 1999; p 1424.

(17) Farrell, J.; Reinhard, M. Desorption of halogenated organics from model solids, sediments, and soil under unsaturated conditions. 1. Isotherms. *Environ. Sci. Technol.* **1994**, *28* (1), 53–62.

(18) Dhingra, O. D.; Sinclair, J. B. *Basic Plant Pathology Methods,* 2nd ed.; CRC Press: Boca Raton, FL, 1995; p 434.

(19) Kleineidam, S.; Rugner, H.; Grathwohl, P. Desorption kinetics of phenanthrene in aquifer material lacks hysteresis. *Environ. Sci. Technol.* **2004**, *38* (15), 4169–4175.

(20) Aylmore, L. A. G. Microporosity in montmorillonite from nitrogen and carbon dioxide sorption. *Clays Clay* Miner. **1977**, *25* (2), 148–154.

(21) Murray, R. S.; Quirk, J. P. Surface area of clays. *Langmuir* **1990**, *6* (1), 122–124.

(22) Sposito, G.; Prost, R.; Gaultier, J. P. Infrared spectroscopic study of adsorbed water on reduced-charge Na/Li-montmorillonites. *Clays Clay Miner.* **1983**, *31* (1), 9–16.

(23) Jaynes, W. F.; Boyd, S. A. Hydrophobicity of siloxane surfaces in smectites as revealed by aromatic hydrocarbon adsorption from water. *Clays Clay Miner.* **1991**, *39* (4), 428–436.

(24) Hundal, L. S.; Thompson, M. L.; Laird, D. A.; Carmo, A. M. Sorption of phenanthrene by reference smectites. *Environ. Sci. Technol.* **2001**, *35* (17), 3456−3461.
(25) Aochi, Y. O.; Farmer, W. J. Role of microstructural properties in the time-dependent sorption/desorption behavior of 1,2-dichloroethane on humic substances. *Environ. Sci. Technol.* **1997**, *31* (9), 2520−2526.
(26) Karapanagioti, H. K.; Kleineidam, S.; Sabatini, D. A.; Grathwohl, P.; Ligouis, B. Impacts of heterogeneous organic matter on phenanthrene sorption: Equilibrium and kinetic studies with aquifer material. *Environ. Sci. Technol.* **2000**, *34* (3), 406−414.
(27) Kleineidam, S.; Schuth, C.; Grathwohl, P. Solubility-normalized combined adsorption-partitioning sorption isotherms for organic pollutants. *Environ. Sci. Technol.* **2002**, *36* (21), 4689−4697.
(28) Macalady, D. L.; Wolfe, N. L. Effects of sediment sorption and abiotic hydrolyses 1. organophosphorothioate esters. *J. Agric. Food Chem.* **1985**, *33* (2), 167−173.
(29) Haag, W. R.; Mill, T. Effect of a subsurface sediment on hydrolysis of haloalkanes and epoxides. *Environ. Sci. Technol.* **1988**, *22* (6), 658−663.
(30) Farrell, J.; Hauck, B.; Jones, M. Thermodynamic investigation of trichloroethylene adsorption in water-saturated microporous adsorbents. *Environ. Toxicol. Chem.* **1999**, *18* (8), 1637−1642.

Received for review November 9, 2005. Revised manuscript received February 21, 2006. Accepted February 23, 2006.

ES0522581